Performance Analysis of Active Intelligent Reflecting Surface-Assisted System: BER and Sum-Rate Evaluation

Sanjeev Sharma, Kuntal Deka, Cédric Adjih, Alok Kumar

Performance Analysis of Active Intelligent Reflecting Surface-Assisted System: BER and Sum-Rate Evaluation

Sanjeev Sharma[1], Kuntal Deka[2], Cedric Adjih[3], and Alok Kumar[4]
[1]IIT (BHU) Varanasi, India, [2]IIT Guwahati, India, [3]INRIA, Frances, and [4]Jaypee University of Information Technology, Waknaghat, India
Email: sanjeev.ece@iitbhu.ac.in, kuntaldeka@iitg.ac.in, cedric.adjih@inria.fr, and alok.kumar@juit.ac.in

***Abstract*—An active intelligent reflecting surface (IRS) has been introduced as a solution to address the *double fading* effect in passive IRS (PIRS)-assisted wireless systems, which is caused by a weak reflection link. The active IRS (AIRS) enhances the received signal strength by amplifying the reflected signal and applying a phase shift at the IRS panel. This paper presents the design and analysis of an AIRS-assisted wireless system, with a focus on examining the bit error rate (BER) and sum-rate performance of the system. Effect of imperfect channel state information, modulation order, the distance between IRS and the receiver, and the total reflected power at the IRS panel is studied. The simulation results demonstrate a significant performance improvement of AIRS compared to PIRS, with an improvement of around 15-20 dB. Unlike PIRS, which does not enhance system performance in the presence of a direct link, AIRS proves to be effective. Moreover, it is observed that a PIRS with an ultra-large number of reflecting elements may achieve performance comparable to AIRS when its total reflected power is lower.**

***Index Terms*—Active intelligent reflecting surface (AIRS), imperfect channel state information (ICSI), signal-to-noise ratio (SNR) maximization, BER, Sum-rate**

I. Introduction

Intelligent reflecting surfaces (IRS)[1] are considered for the next-generation wireless network. IRS can reconfigure the impinged signals toward a desired direction by changing their phases [1, 2]. IRS is a low-cost solution to enhance the coverage area and improve the channel capacity of a wireless system with low power. Therefore, IRS-assisted systems can have higher energy and spectral efficiencies for next-generation networks.

However, the introduction of passive IRS (PIRS) in a wireless system brings about a significant drawback: the occurrence of *multiplicative fading*[2]. This effect notably reduces the gain of the reflection link (Tx-IRS-Rx) in comparison to the direct link. Consequently, when a strong direct link exists between the transmitter (Tx) and receiver (Rx), the capacity improvement of a PIRS-assisted system is minimal. It is worth noting that most existing studies in the literature on IRS-assisted systems have primarily focused on scenarios where the direct link between Tx and Rx is either absent or blocked.

Furthermore, the reflection coefficient of an IRS is also dependent on the phase shift value [3, 4]. In order to overcome the limitations imposed by *multiplicative fading*, an innovative solution called active IRS (AIRS) has recently emerged. This AIRS offers significant enhancements to system capacity, regardless of the strength or presence of the direct link between Tx and Rx. Unlike PIRS, which relies solely on phase-shifting for signal reflection with reflection coefficients less than one, AIRS incorporates a power amplifier in each element of the reflecting surface. This active amplification, combined with phase-shifting capabilities, allows for precise control over the emitted signals from each element [5–7].

By dynamically adjusting the phase and amplitude of the signals emitted by the active elements, the overall signal strength can be greatly enhanced. This leads to improvements in signal-to-noise ratio (SNR), resulting in higher data rates, extended communication ranges, and reduced power consumption. Additionally, the active elements of the IRS can be employed to effectively cancel interference or jamming signals, a capability that is not possible with passive elements alone. Furthermore, it has been demonstrated that AIRS can transform *multiplicative fading* into *additive fading*, further enhancing the system's performance and robustness [8, 9].

AIRS incorporates power amplifiers in each reflecting element, resulting in power consumption that increases with the number of reflecting elements. As the number of elements grows, the power consumption can reach the order of Watts. To address this limitation, a sub-connected AIRS architecture has been proposed in [10]. Recent studies [11, 12] have also analyzed various AIRS-assisted systems. It is important to note that AIRS differs from conventional amplify-and-forward (AF) and decode-and-forward (DF) relays, which rely on power-intensive radio frequency (RF) chains for receiving and transmitting signals. In contrast, AIRS utilizes tunnel diodes that perform instantaneous signal reflection and amplification, eliminating the need for sensing capabilities and RF chains. This RF chain-free architecture significantly reduces power consumption and hardware costs [9].

In the literature [13–19], there is a predominant focus on PIRS-assisted system designs. Some studies explore the application of IRS in low-complexity system designs, such as IRS-space shift keying and IRS-spatial modulation schemes, as discussed in [13]. These designs aim to achieve improved bit error rate (BER) performance. The deployment strategies of IRS are also examined, with centralized and distributed deployments compared in [14]. Centralized deployment generally exhibits superior performance compared to distributed deployment in practical scenarios. Additionally, the impact of self-interference on the performance of IRS-assisted systems is investigated in [[20]. The outage probability (OP) and diversity order of the system are derived for rectangular quadrature amplitude modulation (QAM) and hexagonal QAM schemes.

In [21] a joint active and passive IRS-assisted system is

[1]IRS is also referred to as reflecting intelligent surfaces (RIS).

[2]The pathloss of a Tx-IRS-Rx link is determined by the multiplication of the pathloss of the Tx-IRS link and the IRS-Rx link, rather than their sum.

TABLE I: A Summary of Representative Works on AIRS

Reference	Work	Contribution
[4]	sum-rate maximization	active and passive IRS placement optimization
[8]	sum-rate analysis	performance analysis using active IRSs, which are uniformly deployed within a ring concentric with the cell to serve the users far from the base station
[9]	sum-rate analysis	maximization of the sum-rate of users in the active-IRS-assisted uplink non-orthogonal multiple access (NOMA) system
[5]	sum-rate analysis	multiple active and passive IRS-based system optimization
[6]	sum-rate analysis	SISO-based active IRS-assisted system SNR maximization
[7]	sum-rate analysis	simple beamforming methods are presented

designed. Authors have optimized the position of one IRS by fixing the position of another IRS. The sum-rate performance is plotted for different numbers of the reflecting elements in [21]. In [8] AIRSs are deployed in a cell, and the single nearest IRS is selected by a user for communication. Signal-to-noise ratio (SNR) is examined in an IRS-assisted system in [8]. In [22], multiple PIRSs and a single AIRS are deployed for coverage area enhancement.

In [11] active/passive IRS-assisted system is analyzed by considering e wireless power transfer (WPT)-based energy harvesting. Deep learning (DL)-based system design is considered in [12] for an AIRS-assisted system. Further, an AIRS-assisted NOMA system is studied in [9]. Sum-rate performance is optimized by considering beamforming and reflection coefficients optimization separately. Some AIRS related works are summarized in Table I.

Contributions: This article presents the design and analysis of an AIRS-assisted wireless system. The system's input-output model is formulated to consider both the direct and reflected links. SNR expressions are derived for both single input single output (SISO) and multiple input single output (MISO) scenarios. The BER and sum-rate performance are evaluated numerically. The results indicate a significant improvement in system performance when utilizing AIRS, compared to PIRS, with a gain of approximately 15-20 dB. Additionally, the impact of distance, imperfect channel state information, modulation order, and the total reflected power is studied in the AIRS-assisted system. In the presence of a direct link, PIRS does not provide a significant improvement in system performance, unlike AIRS. Therefore, this paper highlights the strengths and weaknesses of active and passive IRS-assisted systems.

Notations: Bold small and capital letters represent the vector and matrix, respectively. $\mathbb{C}$ denotes the complex number. $\mathcal{CN}(\mu, \sigma^2)$ denotes the complex Gaussian distribution with mean μ and variance σ^2. $|(\cdot)|$ and $||(\cdot)||$ are the absolute value and the Euclidean norm, respectively. $\mathbb{E}[(\cdot)]$ denotes the statistical expectation. Term diag$(\cdot)$ denotes the diagonal matrix generated by a vector and diag$^{-1}(\cdot)$ represents a vector corresponding the diagonal matrix.

II. Active IRS System Model

In this section, the AIRS-assisted wireless system model is described. Tx consists of N_t antennas and Rx has a single antenna. Both the direct and the reflected (via IRS) links exit between the Tx and Rx, as shown in Fig. 1.

The transmitted signal vector $\mathbf{x}$ is expressed as

$$\mathbf{x} = \sqrt{P}\mathbf{w}x \in \mathbb{C}^{N_t \times 1}, \tag{1}$$

where $\mathbf{w} \in \mathbb{C}^{N_t \times 1}$ denotes the beamforming vector. P is the transmit power per symbol and x represents the constellation points corresponding to the information bits with $\mathbb{E}[||x||^2] = 1$. The received signal at the IRS is expressed as

$$\mathbf{x}_{\mathrm{I}} = \mathbf{H}\mathbf{x} \in \mathbb{C}^{N \times 1}, \tag{2}$$

where $\mathbf{H} \in \mathbb{C}^{N \times N_t}$ denotes the channel matrix between the Tx and IRS panel.

An AIRS panel consists of PIN diodes and amplifiers, hence it generates the noise. The reflected signal at the AIRS is expressed as

$$\mathbf{y}_{\mathrm{I}} = \mathbf{\Psi}\mathbf{H}\mathbf{x} + \mathbf{\Psi}\mathbf{n}_a \in \mathbb{C}^{N \times 1}, \tag{3}$$

where $\mathbf{\Psi}\mathbf{n}_a$ is the amplified noise by the AIRS panel. $\mathbf{\Psi}$ is the IRS panel response matrix of size $N \times N$, and $\mathbf{\Psi}\mathbf{H}\mathbf{x}$ is the amplified desired signal towards the Rx. The average total reflected power by IRS is expressed as

$$\begin{aligned} P_{\mathrm{I}} &= \mathbb{E}[(\mathbf{\Psi}\mathbf{H}\mathbf{x} + \mathbf{\Psi}\mathbf{n}_a)^H(\mathbf{\Psi}\mathbf{H}\mathbf{x} + \mathbf{\Psi}\mathbf{n}_a)] \\ &= P\mathbb{E}[(\mathbf{\Psi}\mathbf{H}\mathbf{w}x)^H(\mathbf{\Psi}\mathbf{H}\mathbf{w}x)] + \mathbb{E}[(\mathbf{\Psi}\mathbf{n}_a)^H(\mathbf{\Psi}\mathbf{n}_a)] \\ &= P\mathbb{E}[(\mathbf{\Psi}\mathbf{p}x)^H(\mathbf{\Psi}\mathbf{p}x)] + \sigma_I^2\boldsymbol{\psi}^H\boldsymbol{\psi} \\ &= P\mathbf{p}^H\mathbf{\Psi}^H\mathbf{\Psi}\mathbf{p} + \sigma_I^2\boldsymbol{\psi}^H\boldsymbol{\psi} \\ &= P\sum_{n=1}^{N}|p(n)\psi(n)|^2 + \sigma_I^2\sum_{n=1}^{N}|\psi(n)|^2, \end{aligned} \tag{4}$$

where $\mathbf{p} = \mathbf{H}\mathbf{w}$ and $\boldsymbol{\psi} = \mathrm{diag}^{-1}(\mathbf{\Psi})$. The $p(n)$ and $\psi(n)$ denote the nth entry of the $\mathbf{p}$ and $\boldsymbol{\psi}$, respectively. The diagonal matrix $\mathbf{\Psi}$ is generated using vector $\boldsymbol{\psi} = [a_1 e^{j\phi_1}, a_2 e^{j\phi_2}, ..., a_N e^{j\phi_N}]^T$ as $\mathbf{\Psi} = \mathrm{diag}(\psi)$, where a_n and ϕ_n are the reflection coefficient and phase of the nth reflecting element, respectively. The values of reflection coefficients are generated using the total reflected power P_I of the IRS[3].

[3]In the passive IRS case, $a_n = 1, \forall n$ is used.

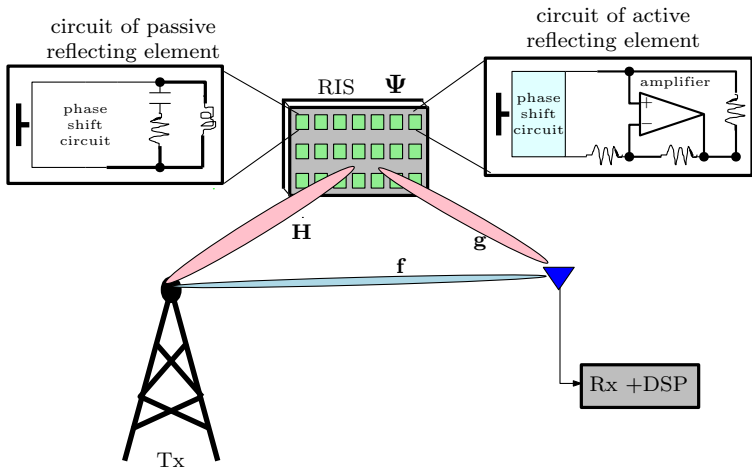

Fig. 1: IRS-assisted wireless system. Rx receives the signal from both the direct ($\mathbf{f}$) and reflected ($\mathbf{g}^T\mathbf{\Psi}\mathbf{H}$) links. $\mathbf{\Psi}$ denotes the response of the IRS panel. Active elements need power supply for amplification, unlike passive elements.

Therefore, AIRS optimizes both the reflection coefficient and phase of each element. By considering the reflection coefficient of each element is the same, the vector $\boldsymbol{\psi}$ can be expressed as $\boldsymbol{\psi} = \lambda\tilde{\boldsymbol{\psi}}$, where $||\tilde{\boldsymbol{\psi}}|| = 1$ and $||\boldsymbol{\psi}|| = \lambda$.
The received signal y at Rx is expressed as

$$\begin{aligned} y &= \mathbf{f}^H\mathbf{x} + \mathbf{g}^H\mathbf{\Psi}\mathbf{x}_I + \mathbf{g}^H\mathbf{\Psi}\mathbf{n}_a + n \\ y &= \sqrt{P}[\mathbf{f}^H\mathbf{w} + \mathbf{g}^H\mathbf{\Psi}\mathbf{H}\mathbf{w}]x + \mathbf{g}^H\mathbf{\Psi}\mathbf{n}_a + n, \end{aligned} \tag{5}$$

where $\mathbf{\Psi} \in \mathbb{C}^{N\times N}$ is a diagonal matrix, and it represents the response of the AIRS. $\mathbf{n}_a \in \mathbb{C}^{N\times 1}$ and n denote the additive white Gaussian noise (AWGN) at the IRS and Rx, respectively. Since AIRS uses an amplifier and phase shifting mechanism, which also introduces the noise in the system. IRS noise $\mathbf{n}_a$ is modeled as $\mathbf{n}_a \sim \mathcal{N}(0, \sigma_I^2\mathbf{I}_N)$. The AWGN at the Rx is modeled as $n \sim \mathcal{N}(0, \sigma_I^2)$. $\mathbf{f} \in \mathbb{C}^{N_t\times 1}$ and $\mathbf{g} \in \mathbb{C}^{N\times 1}$ denote the channel vector between Tx-Rx and IRS-Rx links, respectively. AIRS noise is amplified and received as $\mathbf{g}^H\mathbf{\Psi}\mathbf{n}_a$. Therefore, total noise power at the Rx is given as

$$P_n = \mathbb{E}[(\mathbf{g}^H\mathbf{\Psi}\mathbf{n}_a + n)^H(\mathbf{g}^H\mathbf{\Psi}\mathbf{n}_a + n) = \sigma_I^2||\mathbf{g}||^2||\boldsymbol{\psi}||^2 + \sigma_n^2. \tag{6}$$

The SNR at the Rx is expressed as

$$\text{SNR} = P\frac{||\mathbf{f}^H\mathbf{w} + \mathbf{g}^H\mathbf{\Psi}\mathbf{H}\mathbf{w}||^2}{\sigma_I^2\boldsymbol{\psi}^H\mathbf{g}\mathbf{g}^H\boldsymbol{\psi} + \sigma_n^2} = P\frac{||\tilde{\mathbf{f}}^H\mathbf{w}||^2}{\sigma_I^2\boldsymbol{\psi}^H\mathbf{g}\mathbf{g}^H\boldsymbol{\psi} + \sigma_n^2}, \tag{7}$$

where $\tilde{\mathbf{f}}^H = \mathbf{f}^H + \mathbf{g}^H\mathbf{\Psi}\mathbf{H} \in \mathbb{C}^{1\times N_t}$ is the equivalent channel from the Tx to the Rx, which includes both the direct link and the reflected link. Therefore, SNR maximization is formulated as

$$\begin{aligned} &\max_{\mathbf{\Psi},\mathbf{w}} \ \text{SNR} \\ &C_1 : P||\mathbf{w}||^2 \le P_{Tx} \\ &C_2 : P\sum_{n=1}^{N}|p(n)\psi(n)|^2 + \sigma_I^2\sum_{n=1}^{N}|\psi(n)|^2 \le P_I \end{aligned} \tag{8}$$

In the above optimization problem, the power constraints at the Tx and AIRS are denoted as C_1 and C_2, respectively. However, due to the non-convex nature and strong interdependence among variables, the joint design of $\mathbf{\Psi}$ and $\mathbf{w}$ becomes challenging in this optimization problem. Therefore, we consider only single input and a single output (SISO) system design henceforth in the paper.

A. Active IRS-assisted SISO System

In this section, the SISO-based ($N_t = 1$) AIRS system is analyzed to optimize the SNR of the received signal for simplicity. For SISO system ($\mathbf{H} = \mathbf{h}$), the received signal using (5) is given as

$$\tilde{y} = \sqrt{P}[f + \mathbf{g}^H\mathbf{\Psi}\mathbf{h}]x + \mathbf{g}^H\mathbf{\Psi}\mathbf{n}_a + n, \tag{9}$$

The total received signal power is given as

$$\mathbb{E}[\tilde{y}^H\tilde{y}] = P||(f + \mathbf{g}^H\mathbf{\Psi}\mathbf{h})||^2 + \sigma_I^2||\mathbf{g}||^2||\boldsymbol{\psi}||^2 + \sigma_n^2. \tag{10}$$

Total reflected power at the IRS is expressed as

$$\begin{aligned} P_I &= \mathbb{E}[(\mathbf{\Psi}\mathbf{h}x + \mathbf{\Psi}\mathbf{n}_a)^H(\mathbf{\Psi}\mathbf{h}x + \mathbf{\Psi}\mathbf{n}_a) \\ &= P\mathbf{h}^H\mathbf{\Psi}^H\mathbf{\Psi}\mathbf{h} + \sigma_I^2\boldsymbol{\psi}^H\boldsymbol{\psi} \end{aligned} \tag{11}$$

Using $\boldsymbol{\psi} = \lambda\tilde{\boldsymbol{\psi}}$, the above (11) is expressed as

$$\begin{aligned} P_I &= P\boldsymbol{\psi}^H\mathbf{H}_1^H\mathbf{H}_1\boldsymbol{\psi} + \sigma_I^2\boldsymbol{\psi}^H\boldsymbol{\psi} \\ &= P\lambda^2\tilde{\boldsymbol{\psi}}^H\mathbf{H}_1^H\mathbf{H}_1\tilde{\boldsymbol{\psi}} + \lambda^2\sigma_I^2\tilde{\boldsymbol{\psi}}^H\tilde{\boldsymbol{\psi}}. \end{aligned} \tag{12}$$

Therefore, term λ is calculated as

$$\lambda = \sqrt{\frac{P_I}{P\tilde{\boldsymbol{\psi}}^H\mathbf{H}_1^H\mathbf{H}_1\tilde{\boldsymbol{\psi}} + \sigma_I^2\tilde{\boldsymbol{\psi}}^H\tilde{\boldsymbol{\psi}}}} \tag{13}$$

where $\mathbf{H}_1$ is the diagonal matrix corresponding vector $\mathbf{h}$, i.e., $\mathbf{H}_1 = \text{diag}(\mathbf{h})$. Further, SNR is expressed as

$$\text{SNR} = P\frac{||f + \mathbf{g}^H\mathbf{H}\boldsymbol{\psi}||^2}{\sigma_I^2\boldsymbol{\psi}^H\mathbf{g}\mathbf{g}^H\boldsymbol{\psi} + \sigma_n^2} = P\frac{||f + \lambda\mathbf{g}^H\mathbf{H}\tilde{\boldsymbol{\psi}}||^2}{\sigma_I^2\lambda^2\tilde{\boldsymbol{\psi}}^H\mathbf{g}\mathbf{g}^H\tilde{\boldsymbol{\psi}} + \sigma_n^2} \tag{14}$$

The value of λ can be obtained from (13) and the phase is optimized similarly as in PIRS [23].

The received SNR of the SISO system assisted by an IRS is plotted in Fig. 2 and Fig. 3, where the distance of the IRS-Rx link is varied. It is important to note that there is no direct link present in both Fig. 2 and Fig. 3. The channel between the Tx-IRS and IRS-Rx follows Rician fading with a Rician factor of unity. Path loss is determined according to the 3GPP standard [24] models, and additional simulation details can be found in the dedicated simulation section. The Tx and IRS are located at coordinates $[0, -10, 0]$ and $[30, 10, 0]$, respectively. The Rx coordinate varies from $[5, 0, 0]$ to $[50, 0, 0]$ while keeping the y and z coordinates fixed. The transmit power is set to 50 dBm, and perfect phase cancellation at the IRS is employed. In Fig. 2, the received SNR for the AIRS remains relatively constant compared to the PIRS, regardless of the number of reflecting elements. Since the total reflected power is fixed at 10 dBm, the amplification factor decreases as the value of N increases. Furthermore, it can be observed in Fig. 2 that the received signal power for the PIRS case increases as N increases.

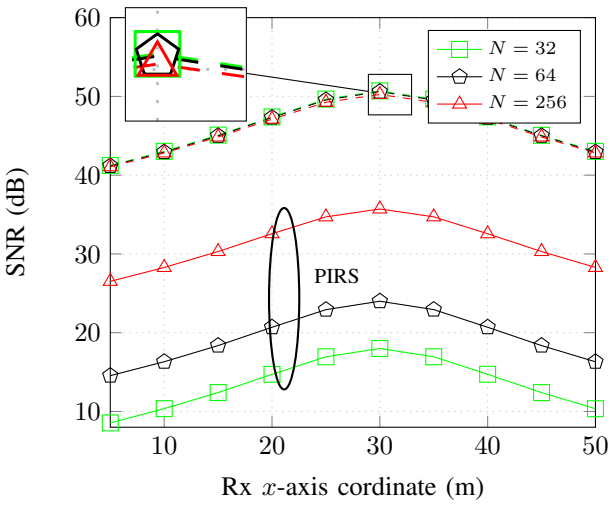

Fig. 2: Average SNR of active/passive IRS-assisted system for different number of reflecting elements N with fixed reflected power.

In Fig. 3, the reflected power is fixed as $N * 10$ dBm, while the total power of the system (including the transmitter power and amplifier power) remains the same for both active and PIRS systems. The received power increases, as the number of reflecting elements increases, as shown in Fig. 3. Therefore, for a large number of N total reflected power also increases. Hence, a small number of reflecting elements are desirable in the AIRS design, unlike PIRS. Furthermore, if the total reflected power is fixed for all values of N, the performance of the PIRS may surpass that of the AIRS, as observed in Fig. 2, which aligns with the findings in [24].

III. Results and Discussion

In this section, AIRS-assisted system performance is numerically computed and is compared to PIRS-based system.

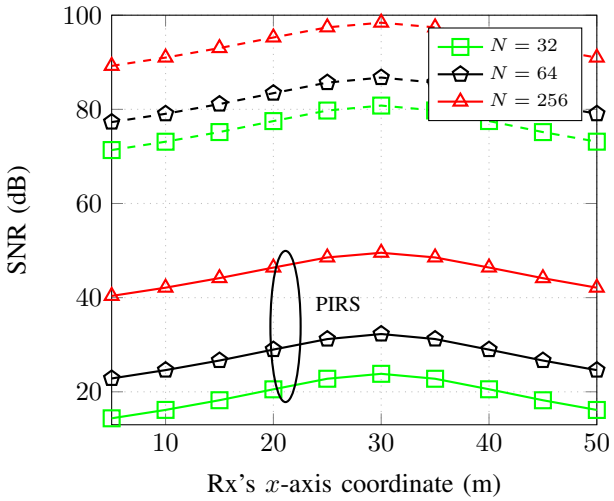

Fig. 3: Average SNR of active/passive IRS-assisted system with $N * 10$ dBm reflected power.

Channel impulse responses (CIRs) between Tx-IRS, IRS-Rx, and Tx-Rx links are generated using the Rician fading as

$$\mathbf{ch} = \sqrt{\frac{k}{k+1}}\mathbf{ch}_{\text{LoS}} + \sqrt{\frac{1}{k+1}}\mathbf{ch}_{\text{NLoS}}, \tag{15}$$

where $\mathbf{ch} = \mathbf{h}, \mathbf{f}, \mathbf{g}$ and k is the Rician factor, which is consider one in simulations. The terms $\mathbf{ch}_{\text{LoS}}$ and $\mathbf{ch}_{\text{NLoS}}$ represent the deterministic line-of-sight (LoS) and non-line-of-sight (NLoS) components, respectively. The path loss for the Tx to IRS and IRS to Rx (IRS-Rx) links is generated using the $37.3 + 22.0 \log_{10} d$ dB model, where d (in m) denotes the distance of the link. Additionally, the path loss for the Tx to Rx (Tx-Rx) link is generated using the $41.2 + 28.7 \log_{10} d$ dB model. The distances for the Tx-IRS, IRS-Rx, and Tx-Rx links are 120 m, 30 m, and 140 m, respectively. Furthermore, binary phase shift keying (BPSK) modulation is used in simulations.

Fig. 4 and Fig. 5 illustrate the BER performance of the IRS-assisted system. In both figures, the total reflected power is set to 10 dBm, the noise power spectral density is -140 dBm, and the system bandwidth is 40 MHz. Fig. 4 represents a scenario where both the direct and indirect links (via IRS) are available, while the direct link is blocked in Fig. 5. Across both figures, the AIRS consistently outperforms the PIRS for all values of N. Moreover, it can be observed that the value of N does not impact the BER performance of the PIRS system when a direct link is present, as depicted in Fig. 4.

Fig. 6 and Fig. 7 demonstrate the average sum-rate performance. It can be observed that the AIRS outperforms the PIRS, as evidenced by the results presented in Fig. 6 and Fig. 7. The AIRS achieves an enhanced sum-rate of approximately 46%, as shown in Fig. 6. Furthermore, when a direct link is present, the sum-rate of the PIRS remains relatively unchanged with varying parameter N, as depicted in Fig. 6. Hence, the AIRS can be employed to achieve higher throughput and extend the coverage area. Conversely, in the presence of a direct link between the Tx and the Rx, the PIRS does not significantly enhance system performance, unlike the AIRS, as illustrated

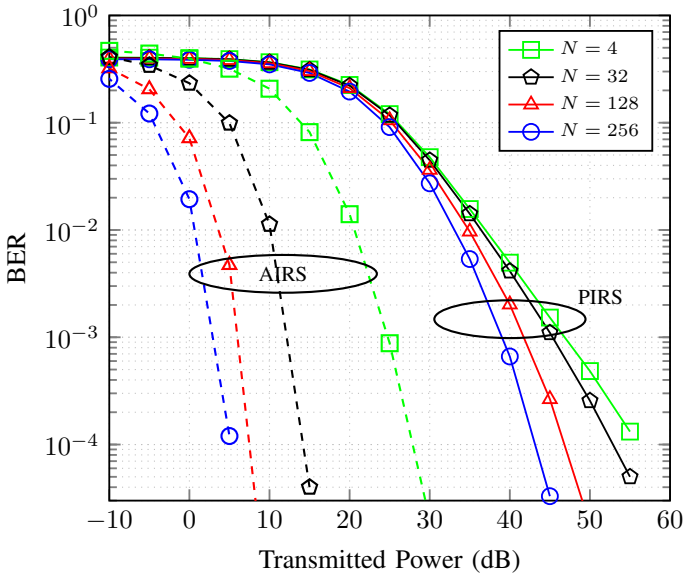

Fig. 4: Average BER performance of active/passive IRS-assisted system for different number of reflecting elements N.

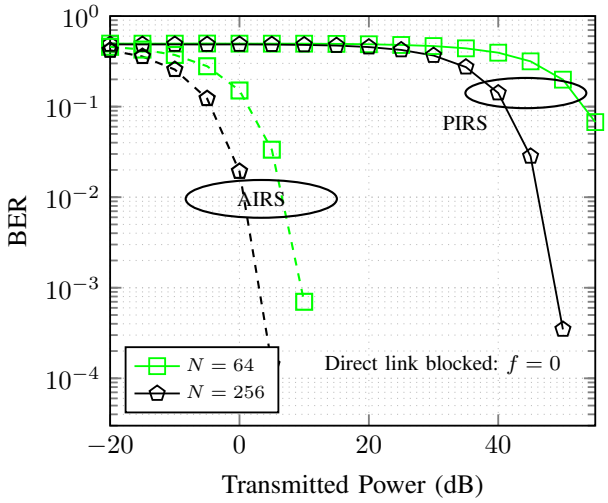

Fig. 5: Average BER performance of active/passive IRS-assisted system for different the number of reflecting elements N when a direct link between Tx and Rx is blocked.

in Fig. 7.

Imperfect CIR: Effect of imperfect CIR is highlighted in Fig. 8 on the BER performance. In practice CIR $\mathbf{h}$ of a link is expressed as

$$\mathbf{h} = \tilde{\mathbf{h}} + \mathbf{e} \tag{16}$$

$\tilde{\mathbf{h}}$ denotes the imperfect CIR and $\tilde{\mathbf{e}}$ is the channel estimation error with $\tilde{\mathbf{e}} \sim \mathcal{CN}(0, \Omega_e \mathbf{I}_N)$. The variance Ω_e is calculated as $\Omega_e = \frac{\Omega_h}{1+\delta \text{SNR}_{Tx} \Omega_h}$, where Ω_h is the variance of the perfect channel $\mathbf{h}$. SNR_{Tx} is the transmitted SNR and δ is the channel estimation quality. $\delta = \infty$ denotes the perfect channel estimation. Further, as SNR_{Tx} increases, channel estimation improves as observed in (16). BER deteriorates into imperfect channel ($\delta = 10^{-2}, 10^{-4}$) scenario as compared to perfect case ($\delta = \infty$), as observed in Fig. 8. In addition, impact of an

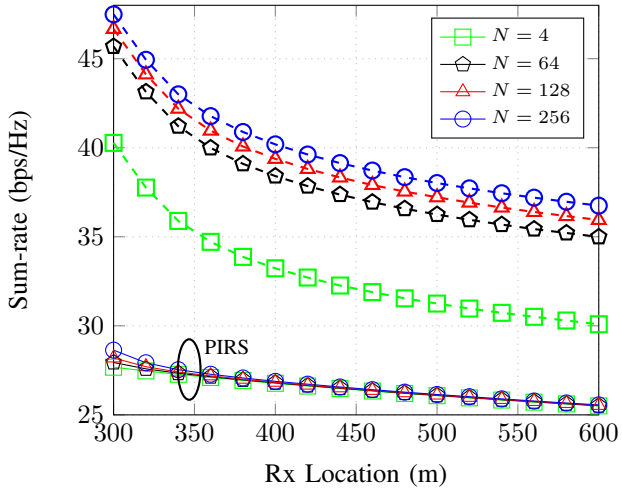

Fig. 6: Average sum-rate performance of active/passive IRS-assisted system for different the number of reflecting elements N. The Tx and IRS are located at $[0, -60, 0]$ and $[300, 10, 0]$, respectively, and Rx location varies from $[300, 0, 0]$ to $[600, 0, 0]$.

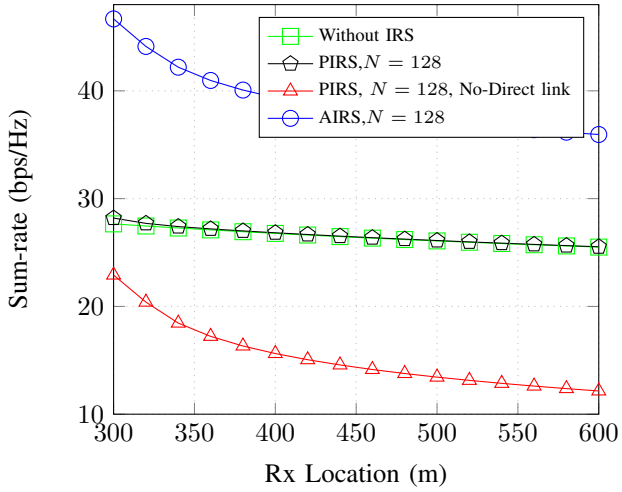

Fig. 7: Average sum-rate performance of active/passive IRS-assisted system.

imperfect channel is higher in AIRS than the PIRS system.

Impact of modulation order: Fig. 9 examines the impact of modulation order (M-ary QAM [25]) and imperfect channel state information. It is observed that the BER performance worsens as the modulation order increases. Particularly, higher-order modulation schemes ($M = 128$) are significantly affected in the presence of an imperfect channel scenario, as shown in Fig. 9.

IV. Conclusion

In this paper, an active IRS (AIRS)-assisted wireless system is designed and analyzed to mitigate the *double fading* effect experienced by passive IRS (PIRS). The BER and sum rate performances of the AIRS-assisted system are numerically evaluated and compared with those of the PIRS. The results indicate a gain of around 15-20 dB at a fixed BER when utilizing the AIRS, as observed in the above results. The impact of a direct link, imperfect channel state information, and modulation order is also investigated. The results demon-

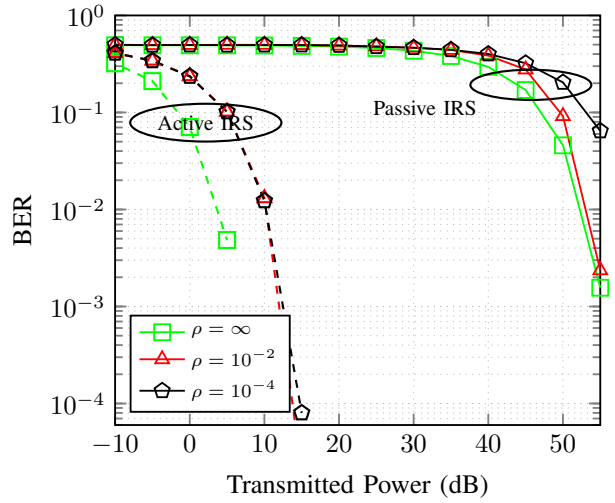

Fig. 8: Average BER performance of active/passive IRS-assisted system in the presence of imperfect CIR scenario for $N = 128$.

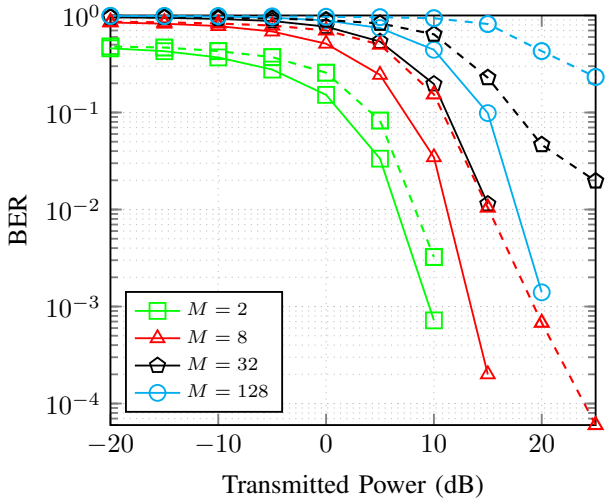

Fig. 9: Average BER performance of AIRS-assisted system for different modulation order M. Solid and dashed lines denote the performance in the presence of perfect and imperfect channel scenarios, respectively for $N = 64$.

strate that in the presence of a direct link, the PIRS does not significantly improve system performance, unlike the AIRS. The AIRS is generally more effective when a lesser number of reflecting elements are used, whereas the PIRS is more advantageous when a larger number of reflecting elements are employed within the IRS system. Therefore, the application of active and passive IRS can be utilized in different scenarios.

ACKNOWLEDGEMENT

The authors would like to thank SERB, Govt. of India, IIT (BHU) Varanasi, IIT Guwahati, INRIA France, and JUIT Solan for all the support. This research is supported by Ministry of Science and Technology, SERB under Grant CRG/2023/005095 and Indian National Academy of Engineering (INAE) Project with Sanction No. 2023/IN-TW/10.

REFERENCES

[1] A. Thomas, K. Deka, S. Sharma, and N. Rajamohan, "IRS-Assisted OTFS System: Design and Analysis," *IEEE Trans. on Veh. Technol.*, vol. 72, no. 3, pp. 3345–3358, 2023.

[2] S. Sharma, K. Deka, Y. Hong, and D. Dixit, "Intelligent reflecting surface-assisted uplink SCMA system," *IEEE Commun. Lett.*, vol. 25, no. 8, pp. 2728–2732, 2021.

[3] H. Lu, Y. Zeng, S. Jin, and R. Zhang, "Delay alignment modulation for multi-IRS aided wideband communication," *arXiv preprint arXiv:2210.10241*, 2022.

[4] C. You and R. Zhang, "Wireless communication aided by intelligent reflecting surface: Active or passive?" *IEEE Wireless Commun. Lett.*, vol. 10, no. 12, pp. 2659–2663, 2021.

[5] Y. Zhang, C. You, and B. Zheng, "Multi-active multi-passive (MAMP)-IRS aided wireless communication: A multi-hop beam routing design," *IEEE J. on Sel. Areas in Commun.*, 2023.

[6] Y. Lin, F. Shu, R. Dong, R. Chen, S. Feng, W. Shi, J. Liu, and J. Wang, "Enhanced-rate iterative beamformers for active IRS-assisted wireless communications," *IEEE Wireless Commun. Lett.*, 2023.

[7] F. Shu, J. Liu, Y. Lin, Y. Liu, Z. Chen, X. Wang, R. Dong, and J. Wang, "Three high-rate beamforming methods for active IRS-aided wireless network," *IEEE Trans. on Veh. Technol.*, 2023.

[8] Y. Li, C. You, and Y. J. Chun, "Active-IRS aided wireless network: System modeling and performance analysis," *IEEE Commun. Lett.*, vol. 27, no. 2, pp. 487–491, 2023.

[9] C.-W. Chen, W.-C. Tsai, and A.-Y. Wu, "Low-complexity two-step optimization in active-IRS-assisted uplink NOMA communication," *IEEE Commun. Lett.*, vol. 26, no. 12, pp. 2989–2993, 2022.

[10] K. Liu, Z. Zhang, L. Dai, S. Xu, and F. Yang, "Active reconfigurable intelligent surface: Fully-connected or sub-connected?" *IEEE Commun. Lett.*, vol. 26, no. 1, pp. 167–171, 2021.

[11] L. Cantos and Y. H. Kim, "IRS assisted wireless powered communication: Active or passive?" in *13th International Conference on Information and Communication Technology Convergence (ICTC)*. IEEE, 2022, pp. 184–186.

[12] C. He, Y. Ma, S. Huang, and J. Li, "Research on active/passive hybrid IRS assisted communication method based on deep learning," in *27th Asia Pacific Conference on Communications (APCC)*. IEEE, 2022, pp. 483–487.

[13] E. Basar, "Reconfigurable intelligent surface-based index modulation: A new beyond MIMO paradigm for 6G," *IEEE Trans. on Commun.*, vol. 68, no. 5, pp. 3187–3196, 2020.

[14] S. Zhang and R. Zhang, "Intelligent reflecting surface aided multiple access: Capacity region and deployment strategy," in *21st International Workshop on Signal Processing Advances in Wireless Communications (SPAWC)*. IEEE, 2020, pp. 1–5.

[15] B. Zheng, C. You, and R. Zhang, "Fast channel estimation for IRS-assisted OFDM," *IEEE Wireless Commun. Lett.*, vol. 10, no. 3, pp. 580–584, 2020.

[16] A. S. de Sena, D. Carrillo, F. Fang, P. H. Nardelli, D. B. da Costa, U. S. Dias, Z. Ding, C. B. Papadias, and W. Saad, "What role do intelligent reflecting surfaces play in multi-antenna non-orthogonal multiple access?" *IEEE Wireless Commun.*, vol. 27, no. 5, pp. 24–31, 2020.

[17] Q. Wu and R. Zhang, "Towards smart and reconfigurable environment: Intelligent reflecting surface aided wireless network," *IEEE Commun. Mag.*, vol. 58, no. 1, pp. 106–112, 2019.

[18] C. Guo, Y. Cui, F. Yang, and L. Ding, "Outage probability analysis and minimization in intelligent reflecting surface-assisted MISO systems," *IEEE Commun. Lett.*, vol. PP, no. PP, pp. 1–4, 2020.

[19] M. Najafi and R. Schober, "Intelligent reflecting surfaces for free space optical communications," *IEEE Global Communications Conference (GLOBECOM)*, pp. 1–7, 2019.

[20] D. Kumar, P. K. Singya, O. Krejcar, K. Choi, and V. Bhatia, "Performance of IRS-aided FD two-way communication network with imperfect SIC," *IEEE Trans. on Veh. Technol.*, 2023.

[21] M. Fu and R. Zhang, "Active and passive IRS jointly aided communication: Deployment design and achievable rate," *IEEE Wireless Communications Letters*, 2022.

[22] Y. Zhang and C. You, "Multi-hop beam routing for hybrid active/passive IRS aided wireless communications," pp. 3138–3143, 2022.

[23] S. Sharma, K. Deka, and V. Bhatia, "Intelligent reflecting surface-aided downlink SCMA," *IEEE Systems Journal*, vol. 17, no. 2, pp. 3204–3211, 2022.

[24] Z. Zhang, L. Dai, X. Chen, C. Liu, F. Yang, R. Schober, and H. V. Poor, "Active RIS vs. passive RIS: Which will prevail in 6G?" *IEEE Trans. on Commun.*, vol. 71, no. 3, pp. 1707–1725, 2023.

[25] D. Dixit, K. C. Joshi, and S. Sharma, "Performance of intelligent reconfigurable surface-based wireless communications using QAM signaling," *arXiv preprint arXiv:2010.00519*, 2020.